Sliding of a single *lac* repressor protein along DNA is tuned by DNA sequence and molecular switching

Alessia Tempestini[1,2,†], **Carina Monico**[1,†], **Lucia Gardini**[1,3], **Francesco Vanzi**[1,4], **Francesco S. Pavone**[1,2,3,5] **and Marco Capitanio**[1,2,*]

[1]LENS—European Laboratory for Non-linear Spectroscopy, Via Nello Carrara 1, 50019 Sesto Fiorentino, Italy,
[2]Department of Physics and Astronomy, University of Florence, Via Sansone 1, 50019 Sesto Fiorentino, Italy,
[3]National Institute of Optics—National Research Council, Largo Fermi 6, 50125 Florence, Italy, [4]Department of Biology, Via Madonna del Piano 6, 50019 Sesto Fiorentino, Italy and [5]International Center of Computational Neurophotonics, Via Nello Carrara 1, 50019 Sesto Fiorentino (FI), Italy

ABSTRACT

In any living cell, genome maintenance is carried out by DNA-binding proteins that recognize specific sequences among a vast amount of DNA. This includes fundamental processes such as DNA replication, DNA repair, and gene expression and regulation. Here, we study the mechanism of DNA target search by a single *lac* repressor protein (LacI) with ultrafast force-clamp spectroscopy, a sub-millisecond and few base-pair resolution technique based on laser tweezers. We measure 1D-diffusion of proteins on DNA at physiological salt concentrations with 20 bp resolution and find that sliding of LacI along DNA is sequence dependent. We show that only allosterically activated LacI slides along non-specific DNA sequences during target search, whereas the inhibited conformation does not support sliding and weakly interacts with DNA. Moreover, we find that LacI undergoes a load-dependent conformational change when it switches between sliding and strong binding to the target sequence. Our data reveal how DNA sequence and molecular switching regulate LacI target search process and provide a comprehensive model of facilitated diffusion for LacI.

INTRODUCTION

The handling of genetic material inside the cell requires constant recognition of specific sequences or DNA features by DNA-binding proteins, whether they be transcription factors regulating gene expression, polymerases finding their promoter or other enzymes acting on DNA at specific sites. The mechanism of target search thus represents a crucial aspect of the function of DNA-binding proteins. In some instances it has been clearly demonstrated that the binding rate to cognate target sequences exceeds by two to three orders of magnitude what could be expected of a simple three-dimensional (3D) diffusion and collision mechanism (1). One of the most studied systems in this regard is the lactose repressor protein (LacI), and its paradigmatic regulatory unit within the bacterial genome, i.e. the lac operon (2). In this system, LacI inhibits transcription of the operon genes by RNA-polymerase upon binding to its target sequences (the operators) located in proximity of the gene promoter. LacI function is allosterically regulated by inducer molecules that modulate the affinity of the repressor for the operator (3). LacI can switch between two conformations, respectively with very high (LacI-R) and very low (LacI-R*) affinity for the operator. While in the absence of the inducer the equilibrium constant between these two states is nearly equal to unity and LacI-R can strongly bind the operator, the inducer drives the equilibrium toward the LacI-R* conformation, decreasing affinity for the operator and thus inhibiting repressor activity. LacI is a tetrameric protein (a dimer of dimers) with a V-shaped appearance in which each dimer is composed by a DNA-binding N-terminal domain, a hinge region, a regulatory domain containing the inducer binding pocket and a C-terminal helix. Transition from LacI-R to LacI-R* is described by a hinge motion where the two N-terminal subdomains rotate with respect to the C-terminal domains, altering their orientation and, thus, preventing complementarity with the operator sequence (4).

Riggs *et al.* measured an association rate of LacI to the operator 100-times faster than allowed by diffusion, in the absence of inducer (1). Such high binding rate is critical for LacI to perform its function in bacteria, especially considering the low abundance of this protein (approximately five copies per cell (5)) and the low probability of finding the operator sequences only by 3D diffusion (5,6). Since

---

these measurements, several mechanisms have been proposed to explain the faster-than-diffusion binding rate of DNA-binding proteins (7). The most accepted to date is the facilitated diffusion model (8), where the protein exhibits free 3D diffusion leading to non-specific encounters with any DNA sequence, upon which the protein loosely interacts with non-cognate sequences and can undergo 1D diffusion along the DNA helix for some distance until dissociation might occur, unless the cognate target is reached. The temporary reduction of dimensionality of diffusion from 3D to 1D during sliding on nonspecific sequences would account for the observed acceleration of target finding (9).

This basic model of target search leaves, however, several open questions. Does transition from DNA search to cognate sequence recognition require protein conformational changes? How do LacI conformational changes and allosteric regulation relate to the target search process? Does DNA sequence play a role during 1D sliding? In this regard, it becomes fundamental to understand the nature of 1D diffusion and its relationship with LacI conformations and allosteric regulation. This assessment requires the ability of measuring protein–DNA interactions on very fast time scales to avoid missing weak interactions and sliding events, which might lead to productive DNA target encounters during the searching process. Single molecule approaches are particularly amenable for the characterization of protein–DNA interactions aiming at the direct measurement of diffusion constants and the characterization of sequence-dependent processes along a DNA molecule (7,10,11). Previously, Wang *et al.* measured the diffusion coefficient of GFP-LacI fusion along stretched DNA molecules by single molecule tracking *in vitro* (12). Elf *et al.* used a LacI-Venus fusion to assess various parameters of LacI–DNA interactions (target search time, residence time) both in living bacteria and *in vitro* (13). Also, other studies *in vivo* showed that LacI slides along nonspecific sequences and it can slide over the operator sequence several times before binding to it (14).

On one hand, although *in vivo* measurements offer a direct view of the protein behavior in the cell, single molecule detection is challenging due to cell autofluorescence, which reduces signal-to-noise ratio and, therefore, the resolution of the measurements. On the other hand, *in vitro* measurements are typically performed at lower than physiological ionic strength to increase the protein residence time on DNA. In both cases, fluorescence detection is vulnerable to photobleaching, which limits the observation time, and low signal, which limits the localization precision attainable in single molecule tracking measurements (15–18). However, nonspecific protein–DNA interactions are dominated by electrostatics, therefore requiring the ability to measure them at physiological salt concentrations and on fast timescales.

We previously developed ultra-fast force-clamp spectroscopy, a technique based on double optical tweezers, to investigate the force-dependence of interactions between a polymer and a single binding protein with sub-millisecond time resolution (19). Here, we extended our technique to study the target search mechanism of LacI with few base-pair spatial resolution. Our method allows detection of protein–DNA interactions and protein sliding under constant force, measurement of sequence-dependent diffusion

coefficient, as well as the possibility to perform repeated measurements on the same molecule under different inducer concentrations. Application of this method to LacI–DNA interaction under physiological salt concentrations revealed how a single LacI molecule switches between different allosterically regulated conformations to activate target search along non-specific DNA sequences, recognition of cognate sequences or inactivation of the repressor.

MATERIALS AND METHODS

Lac repressor, DNA preparation and experiments

Wild-type LacI was expressed and purified as described previously (20). A 10.2-kbp DNA construct was prepared by conventional polymerase chain reaction and cloning techniques, containing the operator O3 in between two copies of the operator O1. The three operators were placed in the center of the DNA construct to maximize the distance between the two optical traps and the DNA sequence probed during the experiments. The O3 operator was separated by 212 and 92 bp from the two O1 operators, respectively. The DNA molecule was labeled with biotins at both ends, to allow the specific binding to the streptavidin-coated microspheres. To this end, the DNA molecule containing the O1-O3-O1 target sequence was digested with PauI and SalI (Fermentas). The two 5′ overhangs created by restriction digestion were filled with biotin-dNTPs (Invitrogen) by the Klenow exo− DNA polymerase (Fermentas). A laminar flow system was used to incubate biological samples, perform buffer exchanges and to efficiently anchor DNA molecules between the two optically trapped beads (1.07 μm streptavidin-coated polystyrene beads, Spherotech). These protocols are described with great detail elsewhere (17). The multichannel flow chamber (capacity of ∼50 μl) was assembled on top of a coverslip previously coated with silica beads (1.21 μm Bangslabs) and nitrocellulose as described previously (21,22). To this end, silica beads dispersed in 1% nitrocellulose-pentyl acetate solution were smeared on the coverslip and allowed to dry before the flow chamber was assembled. LacI was incubated for 3 min at the concentration of 220 nM to bind non-specifically on the nitrocellulose surface. The flow chamber was then incubated with 1 mg/ml bovine serum albumin (Sigma) for 3 min. The DNA, at the concentration of 10 pM, was anchored between the two trapped beads and the presence of a single DNA molecule was tested by force–extension analysis (23). The DNA molecule was pre-tensioned to ∼3 pN. All experiments were performed in 10 mM Tris buffer, 145 mM KCl, 0.1 mM ethylenediaminetetraacetic acid and 0.2 mM DL-Dithiothreitol (DTT), pH 7.4. Under these conditions, less than one in three silica beads interacted with the DNA molecule, providing evidence that the large majority of the beads contained at most one LacI molecule. Given the dissociation constant for LacI dimer-tetramer equilibrium (in the range 10 nM–1 pM (24)), the great majority of the molecule explored were in the tetrameric form. Control experiments were performed in the same conditions but without LacI to probe non-specific interactions. Out of several tens of beads explored in different slides we could not detect any non-specific interaction.

Experiments with isopropyl β-D-1-thiogalactopyranoside (IPTG) were performed in the same buffer plus IPTG 2 mM. First, we recorded interactions of a single LacI molecule with DNA in the absence of IPTG. Then we used the nm-stabilization feedback system (see next section) to keep track of the exact position of the molecular complex, displaced the bead–DNA–bead complex (herein named 'dumbbell') few microns away from the glass pedestal bead, fluxed the IPTG inside the microfluidic chamber, brought back the dumbbell to the previous position with nm accuracy and repeated the recording. The flow velocity was kept low during buffer exchange to avoid pushing the beads out of the trap (we applied a pressure of 30 mbar allowing 1 ml of solution to enter in about 6 min).

Experimental apparatus and ultrafast force-clamp spectroscopy

The experimental apparatus and ultrafast force-clamp spectroscopy are described in detail elsewhere (19,22). Briefly, the experimental setup comprises an inverted optical microscope combined with double optical tweezers and fluorescence microscopy with single-molecule sensitivity. The apparatus is stabilized to less than 1 nm with both passive and active stabilization (17,25). The active nm-stabilization system uses the bead with the LacI molecule as a landmark to determine the sample coordinates and correct for thermal drifts and low-frequency noise by moving piezo translators. The two traps could be moved along the DNA direction by acousto-optic deflectors (AODs) and the position of the trapped beads was measured using quadrant detector photodiodes placed in a plane conjugate to the back focal plane of the condenser (26). The force F applied on each bead was measured from the displacement of the bead from the trap center (x) and from calibration of the trap stiffness (k), as $F = -kx$. Before each experiment, k was calibrated over the entire range of trap positions used for the experiment, with a power spectrum method (27). Trap stiffnesses in the range of 0.03–0.14 pN/nm were used in the experiments. A custom software written in Labview controlled the force-feedback system and data acquisition through an FPGA board (NI-PCI-7830R), running at 200-kHz sample rate.

Data analysis

Analysis of local interactions acquired with ultrafast force-clamp spectroscopy is extensively described elsewhere (19,22,28). Briefly, detection of local interactions was performed on full recordings or subsets that did not show sliding. Position signals under positive and negative forces were separated for independent analysis and used to calculate the dumbbell velocity. Velocity data were Gaussian-filtered with σ values varying from ∼1 ms at low force (∼2 pN) to ∼60 μs at high force (∼7 pN), because of the increasing signal-to-noise ratio with force. An optimal velocity threshold was calculated to separate bound and unbound events that ensured false events below 1% (19). Cumulative frequency distributions of event durations were fitted with a double exponential function that took into account the

fraction of lost events, resulting from the limited time resolution. Long and short interactions were separated with >99% confidence, as previously described, to separately plot the distribution of long and short events along DNA (19). In the range of force explored in our experiments, detachment rates of long and short interactions obtained on the same DNA molecule did not show dependence on the force direction. Therefore, rates obtained under positive and negative forces were averaged together to get the average rates k_1 and k_2 at a given force.

We followed the same analysis procedure in measurements that included sliding. However, our algorithm detected a significant number of false and missed short events (>1%) in these recording. Therefore, we excluded rates of fast interactions (k_2) obtained from measurements containing sliding. In the subset of measurements comparing LacI kinetics with and without IPTG on the same molecules, the large majority of measurements without IPTG showed sliding. To avoid bad estimates of k_2 due to the aforementioned issue, the k_2 without IPTG reported in the text is the one obtained from the entire set of measurements without IPTG that did not show sliding.

Plots of dumbbell velocity versus DNA position were obtained as follows: first, the dumbbell velocity was averaged with a 13 sample-point window (65 μs time-window). Since the dumbbell in the unbound state is moving at about 100 nm/ms (F ∼ 3 pN) and sliding occurs at slower velocity, the dumbbell velocity is sampled with a spatial resolution of <6.5 nm along the DNA sequence. Velocity-position plots were further averaged with a 2000 points Savitzky-Golay smoothing over the DNA oscillation (about 400 nm in the measurements reported here). The smoothing could reduce the spatial resolution in case of insufficient number of sample points. The spatial resolution can be obtained as $13 * 2000 * $ oscillation(nm)/(duration(s) $*$ sample rate(Hz)), that is 6.5 nm when averaging 8 s records. Shorter recordings would give lower resolution. We analyzed record subsets between 9 and 87 s, so that the spatial resolution was always better than 6.5 nm. Records used for calculation of the correlation between records at different time points for the same LacI and DNA complex were between 3 and 10 s with an estimated spatial resolution in the range of 17.3–6.5 nm. Variation of LacI strain with sliding velocity introduces systematic errors in the determination of the relative position of LacI on DNA. Such errors are, however, appreciable in the velocity-position plots only at transition points between sliding and local interactions and at force-inversion points, and negligible in the other cases. We discuss this point in the Supplementary Methods. Calculation of 1D diffusion coefficient from velocity records is also described in Supplementary Methods and Supplementary Figure S1.

Two-step force-dependent model

We developed a two-step kinetic model to fit the force-dependence of LacI detachment rate from the operator $k_1(F)$. The model is based on two bound states, I and O, and one unbound state, U (Supplementary Figure S2). State I is intermediate between sliding and strongly bound to the operator and state O is strongly bound to the opera-

tor. LacI can switch between state I and O and vice-versa with transition rates k_{IO} and k_{OI}, respectively. Detachment can occur from both states I and O with rates k_{IU} and k_{OU}, respectively. All rates depend exponentially on force $k_{ij} = k_{ij}^0 \exp(\frac{d_{ij}F}{k_B T})$, with distance parameters d_{IO}, d_{IU}, d_{OU} >0 and $d_{OI}<0$. Therefore, if $k_{OI}^0 > k_{IO}^0$, LacI spends most of its time in state I at zero force. As the force increases, k_{IO} increases and k_{OI} decreases, so that, above a threshold force, state O becomes more populated than state I. The kinetic model can be solved following Nolting (29) to get the measured detachment rate $k_1(F)$, which depends on the detachment rates k_{IU} and k_{OU} from both bound states I and O and on the transition rates k_{IO} and k_{OI} between them. The probability density function of the bound state ([I]+[O] = 1-[U]) is:

$$f(t) = -C_2 \lambda_1 \exp(-\lambda_1 t) - C_4 \lambda_2 \exp(-\lambda_2 t)$$

where

$$C_2 = \frac{k_{OI} + k_{IO} + k_{OU} - \lambda_1}{\lambda_1 - \lambda_2}$$

$$C_4 = -\frac{k_{OI} + k_{IO} + k_{OU} - \lambda_2}{\lambda_1 - \lambda_2}$$

$$\lambda_{1,2} = \frac{1}{2}\left(a \pm \sqrt{a^2 - 4b}\right)$$

$$a = k_{OI} + k_{IO} + k_{IU} + k_{OU}$$

$$b = k_{OI}k_{IU} + k_{IO}k_{OU} + k_{IU}k_{OU}$$

and where C_2 and C_4 are calculated with initial conditions [U] = [O] = 0, [I] = 1. From the probability density function we can calculate the average lifetime of the bound state:

$$\tau(F) = \frac{k_{OI} + k_{IO} + k_{OU}}{k_{OI}k_{IU} + k_{IO}k_{OU} + k_{IU}k_{OU}}$$

from which we obtain the detachment rate $k_1(F) = 1/\tau(F)$ that is used to fit experimental data. Rates and distance parameters obtained from the fit are described in Supplementary Figure S2.

RESULTS

High-speed optical tweezers for the study of protein–DNA interactions

Our setup is based on double optical tweezers that are used to suspend a single DNA molecule between two optically trapped beads in a 'dumbbell-like' configuration and to place the DNA in the proximity of a single LacI protein (Figure 1A). The DNA construct is 10.2 kilo base pairs (kbp) long, containing two primary operator sequences (O1) in the center, 304 bp apart from each other and one secondary operator sequence in between (O3), 212 and 92 bp from the two O1 operators (Figure 1A). The interaction of LacI with O3 is about three to four orders of magnitude weaker than the primary operator interaction (30). In a fully extended DNA structure, the distance between the two O1 operators corresponds to ~103 nm (304 bp × 0.34

nm/bp) and the distance between O3 and the two O1 operators to ~72 and ~31 nm. A custom-built multichannel flow system is used to sequentially trap two beads in the bead channel, attach a single DNA molecule between the two beads in the DNA channel, and move the dumbbell in the buffer channel for measurement (Figure 1B and 'Materials and Methods' section) (17). After testing the presence of a single DNA molecule by force-extension analysis, DNA is slightly stretched (F ~3 pN) and positioned in the proximity of a third bead stuck on the coverslip, containing a single LacI protein (Figure 1A). A constant force (F_{tot}) is alternatively applied to each trap, following the ultra-fast force-clamp spectroscopy methodology (19). Under these conditions, the dumbbell moves back and forth at constant velocity (v) against the viscous drag from the solution. Therefore, when the two molecules are not bound, position of the traps over time is a triangular wave (indicated as 'unbound' in Figure 1C). As detailed in the next section, whenever an interaction between LacI and DNA occurred, the dumbbell motion was either slowed down or stopped (indicated respectively as 'sliding' and 'local interaction' in Figure 1C). The relative position between the DNA and LacI molecules was stabilized to about 3 bp (1 nm) by a position feedback system that actively corrected sample drifts with a piezo stage (25). We used the nm-stabilization feedback and the multichannel flow system to achieve a precise control of buffer exchange while maintaining the DNA trapped between the two beads on the same LacI molecule. This allowed us to perform measurements on the same DNA–LacI molecules with and without inducer to probe allosteric regulation of LacI at the single molecule level.

A single LacI protein switches between strong binding with operators, weak binding and sliding along the DNA molecule

By using the high-speed optical tweezers assay described in the previous section, we recorded 156 traces (with variable duration, from 100 to 1100 s) obtained from scanning 22 DNA molecules and 54 LacI molecules. All measurements were performed at physiological ionic strength (145 mM KCl) and with forces in the 3–8 pN range.

We observed that a single LacI molecule produced two different classes of interactions. One class of interactions (herein named 'local interactions') was strong enough to stop the dumbbell for a variable amount of time at precise locations along the DNA filament (i.e. the dumbbell velocity dropped to zero, see Figures 1C and 2). In this case, when the molecular bond was formed, the force applied by the optical tweezers F_{tot} was transferred to LacI, which applied an equal and opposite force $F_{\text{LacI}} = -F_{\text{tot}}$. Conversely, the other class (herein named 'sliding') was characterized by a continuous interaction during which the protein was uninterruptedly attached to the DNA and could slide along the molecule. The applied force F_{tot} drove sliding in the direction of the force and the interaction was detected from the change (i.e. the decrease) in the dumbbell velocity (Figure 2B). In this case, we assume that LacI applied a viscous drag force on DNA proportional to the dumbbell velocity $F_{\text{LacI}} = \gamma_{\text{LacI}} \cdot v_{\text{b}}$, where γ_{LacI} is the viscous drag coefficient of LacI on DNA and v_{b} is the dumbbell velocity when bound to LacI. Local interactions were in turn divided
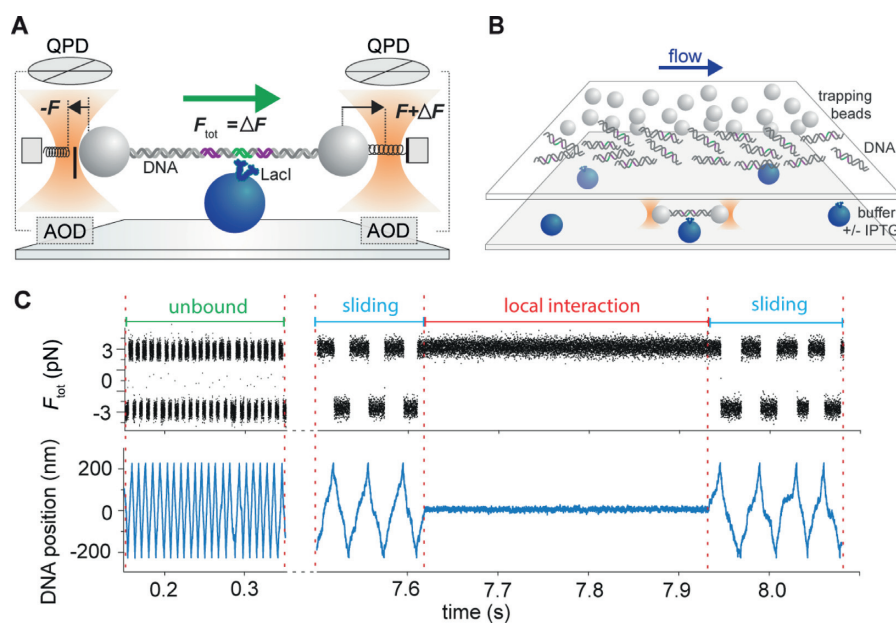
Figure 1. High-speed optical tweezers for the study of protein–DNA interactions. (**A**) A single DNA molecule is suspended between two beads trapped in double optical tweezers. The DNA sequence contains target operator sequences for LacI (two copies of O1, purple, one copy of O3, green). A third bead, stuck on the coverslip, is coated with LacI at single molecule concentration (LacI, blue). A constant force, $F_{tot} = \Delta F$, is alternatively applied to the right and left trap, making the DNA dumbbell move back and forth at constant velocity. The figure shows ΔF applied to the right trap and the corresponding direction of the dumbbell movement (green arrow). Force is kept constant over time by a double force-clamp feedback system, which measures force using quadrant photodiodes (QPD) and rapidly corrects trap positions through AOD. (**B**) A custom-built multichannel flow chamber allows efficient assembly of the molecular construct and buffer exchange. (**C**) Typical ultrafast force-clamp recording during LacI–DNA interaction. Alternating ± 3 pN force (black signal) is applied to the DNA dumbbell, which moves in a ± 200 nm range. Blue signal is the position of the DNA dumbbell versus time. The figure shows different time intervals in which LacI is either detached from the DNA molecule (unbound), sliding on DNA (sliding), or strongly bound to DNA (local interaction).

into either very brief interactions (hundreds of microseconds to tens of milliseconds) or long interactions (of the order of magnitude of seconds to tens of seconds). Sliding varied greatly from molecule to molecule in terms of velocity. Some proteins showed only sliding whereas others only local interactions. However, such variability in the interaction modality was observed not only between different LacI molecules, but also at different times when observing the same molecule, i.e. the protein could switch between short, long and sliding events and *vice versa*, as shown in Figure 2.

We first focused our analysis on the kinetics and binding positions of local interactions. The beginning and the end of each event were detected by the abrupt change in velocity after binding, as previously described (19). In the conditions of the experiments described here, we could detect events as short as about 150 μs. The duration of the events of a typical record is shown in a cumulative frequency graph (Figure 3A). The distribution clearly shows a double exponential behavior, confirming our observation that local interactions comprise two distinct populations characterized by very different detachment kinetics. By fitting those plots with a double exponential function, we obtained the detachment rates of long (k_1) and short (k_2) interactions. Average k_1 and k_2 at 3.0 ± 0.2 pN force are 63.3 ± 13.2 s^{-1} ($n = 106$) and 1149 ± 107 s^{-1} ($n = 44$), respectively (mean value $\pm$ standard error).

We then analyzed how local interactions were distributed along the DNA molecule. Figure 3B shows a typical plot of the duration of events as a function of their binding position

along DNA. Long interactions clearly locate around two precise positions, separated by a distance of about 100 nm from each other, in excellent agreement with the distance between the two O1 operators in our DNA construct. In some measurements, an additional lower peak was observed in the graph at an intermediate position between the two, probably corresponding to the O3 operator. Short interactions appeared instead to be distributed more uniformly along the DNA length.

Since the kinetics of the two detachment rates differ by two orders of magnitude, we could identify and separate the two classes of interactions based on event duration with >99% confidence (see methods). Figure 3C shows how the number of long and short interactions varies along the DNA filament, represented as the fraction or probability that an event occurs at a specific DNA location. As expected, we found that the probability of finding long interactions is tightly peaked around two positions separated by about 100 nm from each other. The width of the two peaks is about 3.5 nm, as expected considering the operator size and thermal noise in the measurement. Surprisingly, we found that also short interactions are more likely to occur in correspondence of the two operators, besides their distribution along all the filament. The width of distribution of these events is wider than for long interactions ($\sim$30 nm for the measurement reported in Figure 3C), but still compatible with the operator size and thermal noise. In fact, on the time scale of short events (ms and sub-ms), the dumbbell can be in any position of the range allowed by thermal noise and
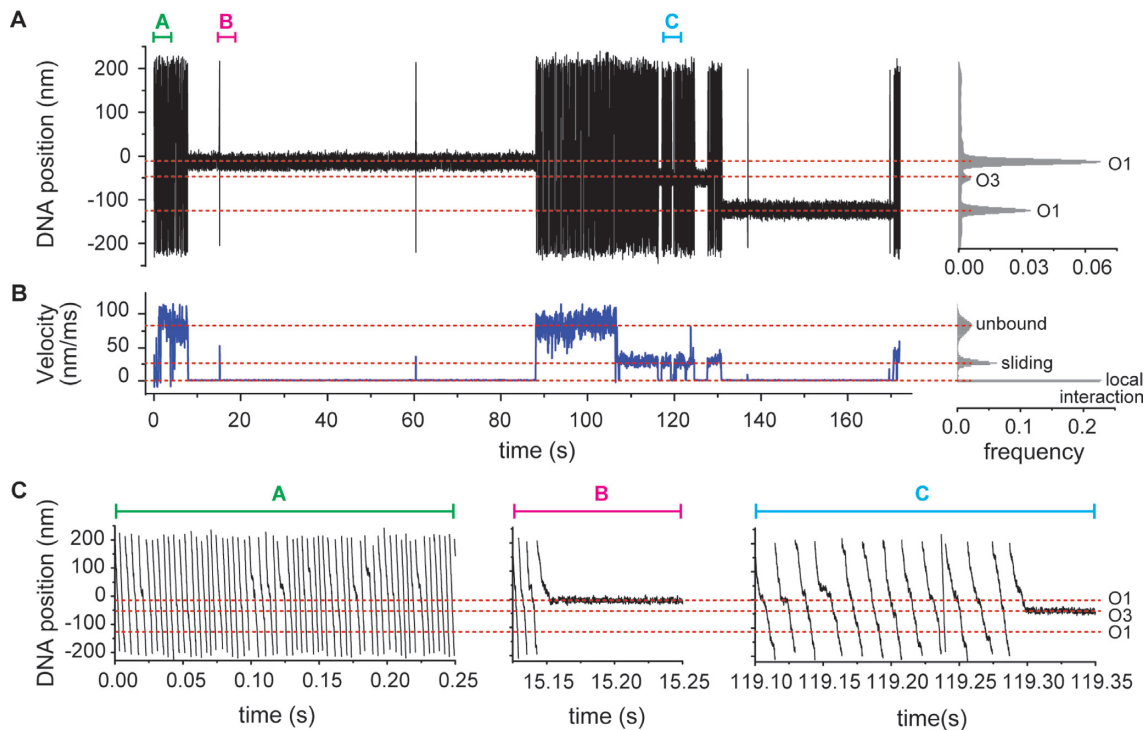
Figure 2. LacI–DNA interactions. (**A**) Left: typical recording of the dumbbell position during LacI–DNA interaction. Right: position histogram. The spacing between long local interactions corresponds to the position of the three operators. Triangular wave is not visible due to the time scale. (**B**) Left: dumbbell velocity obtained from the position record in (A). Right: velocity histogram. In the absence of LacI–DNA interactions, the dumbbell moves at constant velocity (unbound); sliding events slow down the dumbbell (sliding) and local interactions with operators and with non-specific DNA sequences halt the system, as represented by the sharp peak around zero velocity (local interactions). (**C**) Representative position records of three subsets highlighted in panel (A) showing brief local interactions (green, A), switch from unbound to sliding and a long local interaction with O1 (magenta, B) and between sliding and a long local interaction with O3 (cyan, C). In all three panels, only positive forces are displayed. Similar plots are obtained for negative forces (not shown). $F_{tot} = 3$ pN, dumbbell oscillation range is ± 200 nm.
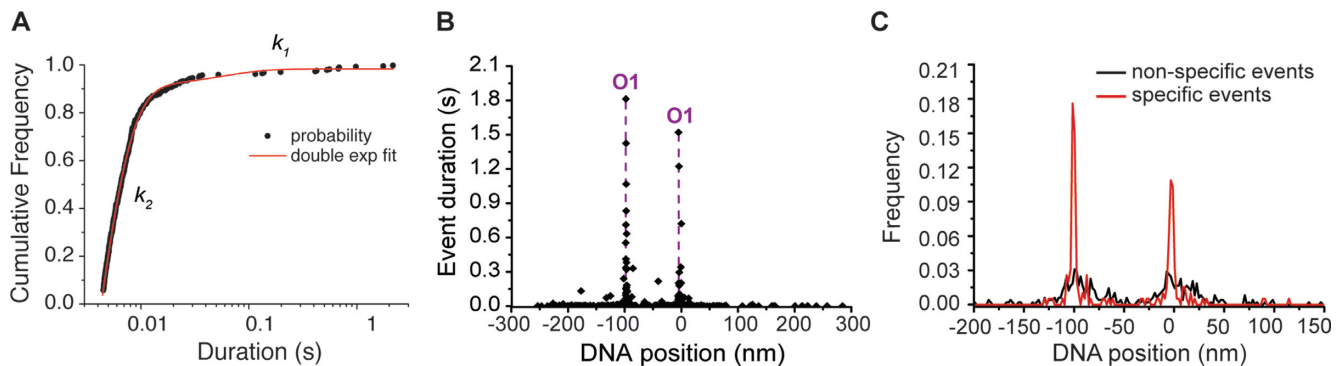

Figure 3. Duration and position of LacI local interactions along DNA. (**A**) Typical cumulative frequency distribution of event duration (black line) and double exponential fit (red line). The two rates k_1 and k_2 obtained from the fit correspond to the detachment rate of long and short events, respectively ($k_1 = 19 \pm 4$ s^{-1}, $k_2 = 368 \pm 3$ s^{-1} for the data shown in figure). (**B**) Duration of events versus DNA position. Long and short interactions can be distinguished along the vertical axis. (**C**) Position histogram of local interactions. Long (red) and short (black) events were separated based on their duration (see methods). $F_{tot} = 3$ pN.

the average position of short events varies broadly around the operator position.

Collectively, these results suggest that long interactions correspond to the binding of LacI in a conformation that strongly binds one of the two O1 operators (LacI-R), whereas short interactions correspond to LacI weakly binding to both specific and nonspecific sequences (LacI-R*). Indeed, the distance between the binding positions during long interactions corresponds to the distance between the two O1 operators, whereas short interactions are spread along the DNA molecule. The very large difference in the detachment kinetics between the two populations further supports the idea that long and short interactions correspond to different LacI conformations with different affinities for DNA.
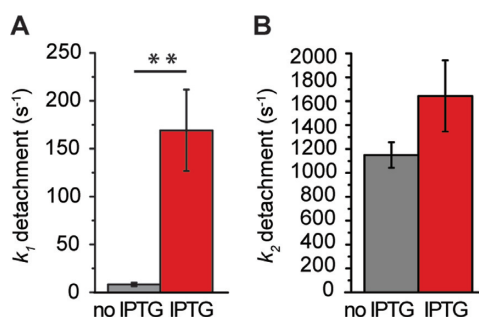
Figure 4. Effect of IPTG on the detachment rates of long (**A**) and short (**B**) local interactions. Both panels represent the average rate before (gray) and after (red) addition of IPTG ($k_1 = 6.4 \pm 1.8$ s^{-1}, $n = 14$ without IPTG, $k_1 = 167 \pm 42$ s^{-1}, $n = 12$ with IPTG; $k_2 = 1149 \pm 107$ s^{-1}, $n = 44$ without IPTG, $k_2 = 1643 \pm 298$ s^{-1}, $n = 9$ with IPTG; error bars = std). Student's t-test applied, **$P < 0.01$. $F_{tot} = 3$ pN.

IPTG accelerates detachment of LacI from cognate sequences but does not affect non-specific interactions

To better understand the nature of long and short local interactions, we performed experiments in the presence of IPTG, an analog of allolactose and an inducer of LacI *in vitro*. IPTG reduces LacI affinity for O1 and accelerates dissociation of LacI from O1 by promoting the low-affinity LacI-R* conformation (3,31). In particular, induced dissociation should play a prominent role at the high IPTG concentrations used here (2 mM). As mentioned above, we could probe the difference in the interaction lifetimes with and without IPTG directly on the same LacI–DNA complex (see also 'Materials and Methods' section).

Cumulative frequency graphs of the duration of events in the presence of IPTG were, again, well fitted by a double exponential function (Supplementary Figure S3). This indicates that two detachment kinetics persist also in the presence of saturating IPTG. Moreover, the populations of long and short interactions were substantially unchanged in the presence of IPTG, their ratio (A_1/A_2) varying from 0.14 ± 0.04 to 0.11 ± 0.05 after addition of IPTG (mean value ± standard error, $n = 44$ and 9, respectively). In Figure 4, we compare the average detachment rates k_1 and k_2 in the presence and absence of IPTG. The slow rate k_1 is significantly different after adding IPTG, varying in this particular set of measurements from an average value of 6.4 ± 1.8 to 167 ± 42 s^{-1} (mean value ± standard error, $n = 14$ and 12 respectively), showing that detachment of long interactions is accelerated about 25-fold by IPTG (P-value = 0.003 from t-test). The rate of short interactions k_2 (1149 ± 107 and 1643 ± 298 s^{-1} without and with IPTG, respectively; mean value ± standard error, $n = 44$ and 9) is instead substantially unchanged, indicating that these events are not affected by the presence of IPTG (P-value = 0.15 from t-test). The accelerated detachment of long interactions in the presence of IPTG strongly supports that long interactions are interactions of LacI-R with the O1 operator sequence, whereas short interactions correspond to the Lac-R* conformation occurring everywhere along the DNA sequence.

Sliding velocity and diffusion coefficient of LacI is modulated by the DNA sequence. IPTG nearly abolishes sliding

In about half of the recordings (72 out of 156), we observed the dumbbell slowing down but not stopping, corresponding to sliding events. The protein could switch from sliding to long interactions at the operator position and *vice versa* (Figure 2 and Supplementary Figure S4). The sliding velocity was very heterogeneous, varying greatly between sliding events: sometimes it was just slightly slower than the dumbbell velocity in the unbound state (in the range 70–90 nm/ms at 3 pN force), while in other cases, it was just a few nm/ms and approaching zero at moments (Figure 5).

It was clear from the recorded traces that the sliding velocity varied along the DNA, with higher and lower sliding velocities correlating with certain DNA positions, which were reproducible in subsequent DNA scans. The variation of the sliding velocity along the DNA suggests a role of DNA sequence in the modulation of the interaction energy with LacI and, consequently, LacI sliding velocity and diffusion coefficient (32). Our experimental configuration allows us to precisely (within ∼7 nm) quantify LacI sliding velocity as a function of DNA sequence, by averaging the dumbbell velocity over several hundreds of DNA scans performed during each recording (see 'Materials and Methods' section). Figure 5B, E and H shows the average sliding velocity as a function of the DNA position for three different recordings acquired on different molecules under the same experimental conditions, corresponding to the three representative traces displayed in panels A, D and G, respectively. Each panel reports the average dumbbell velocity during three different periods of the recording, corresponding to different LacI–DNA interactions: in the unbound state (green), during sliding (cyan) and when the protein switched from sliding to long local interactions (magenta). While the velocity remains essentially constant during the unbound state, the sliding velocity changes greatly between molecules and between different positions on the DNA (Supplementary Figure S6). Velocity of the protein while switching between sliding and long interactions shows zero velocities in correspondence of the two O1 operators and the O3 operator.

Our experimental assay also allows a direct quantification of the diffusion coefficient of a protein sliding along DNA, based on our measurements performed under constant force. In general, the diffusion coefficient can be obtained by the Einstein–Smoluchowski equation as $D = k_B T v / F$, where v is the drift velocity of a protein subjected to a constant force F, k_B is the Boltzmann constant and T the absolute temperature (33). In our setup, the friction force between LacI and DNA sums up with the hydrodynamic drag from the two trapped beads and the DNA molecule. We can determine the contribution of this hydrodynamic drag from the dumbbell velocity in the unbound state and calculate the diffusion coefficient of LacI along DNA as (see Supplementary text):

$$D_{LacI} = \frac{k_B T}{F} \frac{v_b v_u}{v_u - v_b},$$

where v_b and v_u are the velocities of the dumbbell in the bound and unbound state, respectively. Figure 5C, F and
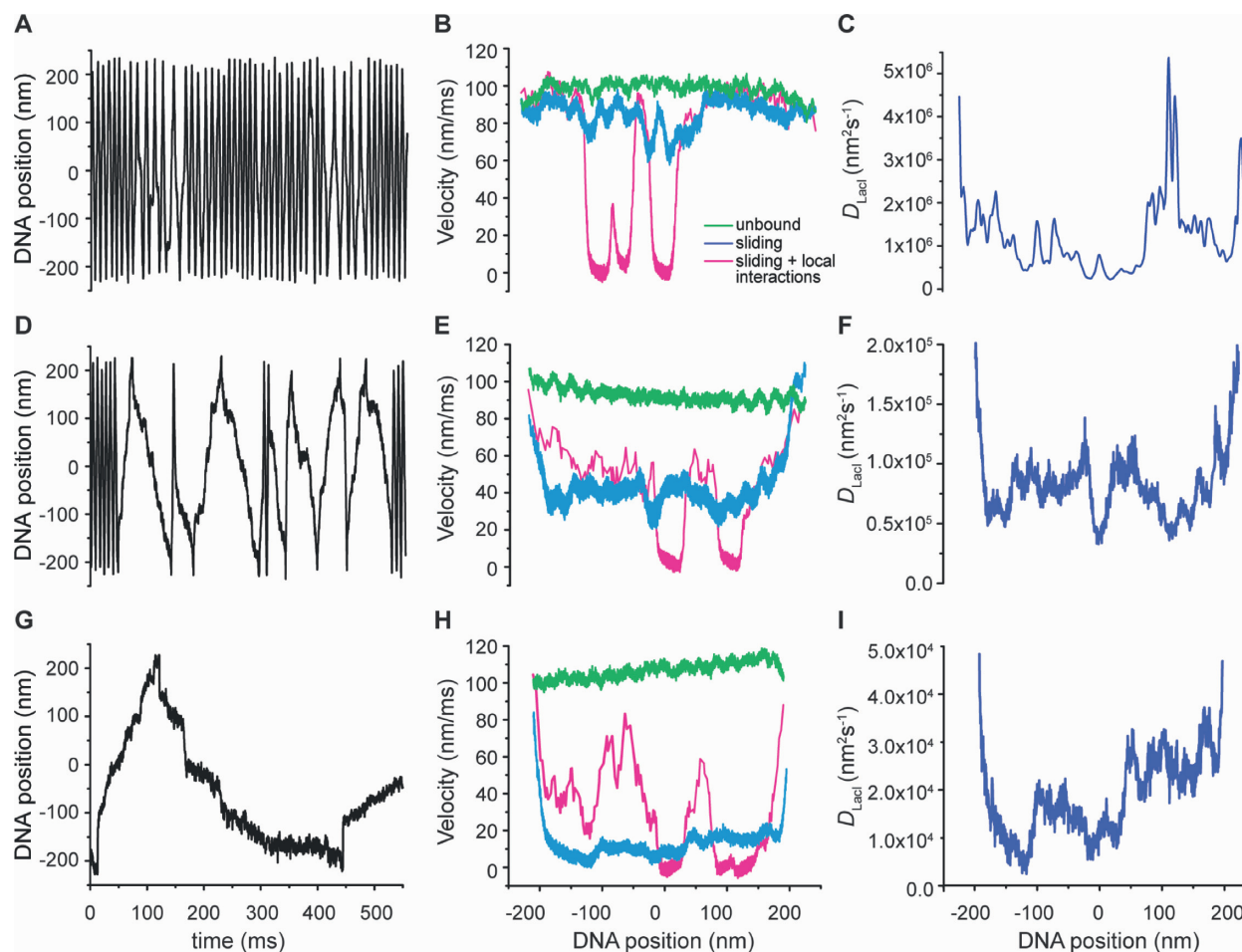
Figure 5. LacI sliding velocity and diffusion coefficient along DNA. Panels **A**, **D** and **G** show three representative recordings of the dumbbell position versus time displaying different sliding velocities (500 ms duration, F_{tot} = 3 pN, dumbbell oscillation range is ±200 nm). Panels **B**, **E** and **H** show the corresponding average dumbbell velocity versus DNA position during: sliding only (cyan); sliding and local interactions (magenta); in the absence of interactions (green). Panels **C**, **F** and **I** show the corresponding LacI diffusion coefficient as a function of DNA position (blue).

I show how the diffusion coefficient varies along the DNA molecule for the three representative traces. We measured 1D diffusion coefficients in the range $1 \cdot 10^4 – 5 \cdot 10^6$ nm^{2}s^{-1}, which are in good agreement with values previously reported from single molecule measurements (12,13). The distribution of diffusion coefficients shows a main peak centered around $(4.1 \pm 2.3) \cdot 10^5$ nm^{2}s^{-1}, error = s.d. (see Supplementary Figure S7).

In our measurements, we observe variations in the diffusion coefficient in different DNA positions as large as ∼300% (Supplementary Figure S6). To figure out whether those variations are due to the DNA sequence, we compared the sliding velocity at different time points for the same LacI and DNA complex while scanning the same DNA segment. We compared 40 pairs of measurement subsets lasting between 3 and 10 s. Figure 6 shows a representative case of one of such pairs. Correlation between the curves was evaluated from the Pearson's r-value, giving 0.82 for the case represented in Figure 6 and an average value of 0.77 ± 0.02 for all the pairs analyzed. Conversely, comparison of measurements obtained from different molecules showed a much lower correlation coefficient (0.19 ± 0.07, $n = 15$), most

probably because the segment of DNA sequence scanned was different and the protein was randomly attached to the bead. The high correlation in LacI sliding velocity with DNA position when comparing the same DNA segment strongly supports the idea that LacI interaction energy and diffusion properties are modulated by DNA sequence (34).

Finally, we compared sliding events before and after adding IPTG. Notably, in 82 min of recordings on 5 LacI molecules, sliding was abolished in 70% of the measurements after addition of 2 mM IPTG and only short interactions that we attributed to the LacI-R* conformation survived. Supplementary Figure S5 shows a representative example in which 1D diffusion was replaced by fast local interactions after addition of IPTG. This finding shows that sliding is mainly due to the Lac-R conformation, whereas Lac-R* induced by IPTG weakly interacts along non-specific DNA sequences and rapidly dissociates from it.

LacI binding to cognate sequence is a catch-bond occurring in two steps

The LacI–DNA complex was subject to different loads by varying the force F_{tot} applied by the optical tweezers to the
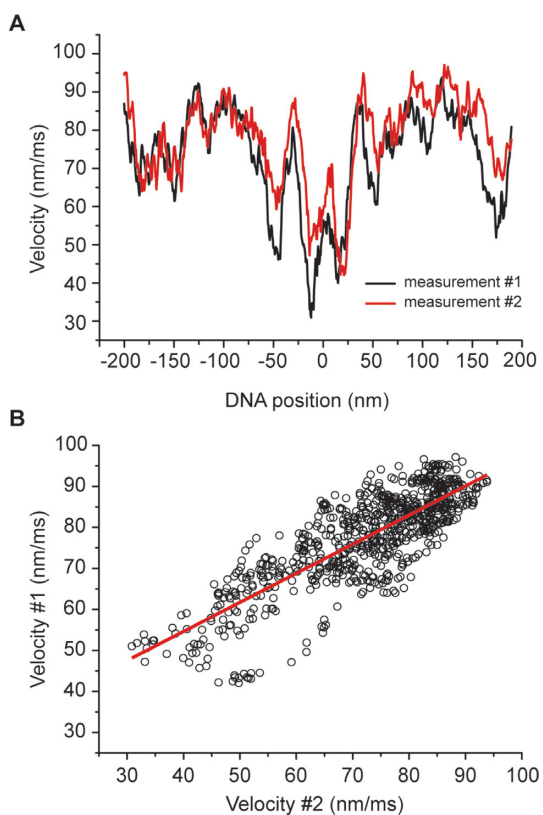
Figure 6. LacI sliding velocity correlates with DNA sequence. (**A**) Average sliding velocity versus DNA position for two recordings (measurement #1 and #2) obtained on the same LacI–DNA segment at different times. (**B**) Correlation analysis of the two measurements shown in panel A. The red curve shows linear regression on the data (black circles): $y = a + bx$, with $a = 26 \pm 1$ nm/ms, $b = 0.71 \pm 0.02$. The Pearson's r-value (0.82) was taken as correlation value.

DNA molecule. Detachment rates of LacI strongly bound to the operator sequence (k_1, Lac-R conformation) and weakly bound to DNA (k_2, Lac-R* conformation) were both accelerated by an external force (Figure 7). However, the force-dependence behavior was remarkably different. The detachment of LacI-R* from DNA was well described by a Bell slip-bond model $k_2(F) = k_2^0 \exp(d_2 F/k_B T)$ (adjusted $R^2 = 0.83$, Figure 7A), which gave a detachment rate at zero force $k_2^0 = 350 \pm 90$ s^{-1} and a distance parameter $d_2 = 1.5 \pm 0.2$ nm. On the other hand, the detachment of LacI-R from the operator could not be fitted accurately by the Bell slip-bond model (adjusted $R^2 = 0.3$, Figure 7B). The detachment rate k_1 showed a behavior typical of catch-bonds, in which the rate increased for low forces (<3 pN), decreased in an intermediate force regime (3 pN < F < 6 pN), and then increased again for forces above 6 pN. Such behavior can be explained by a two-step model in which detachment from the two states follows a slip-bond behavior, but force favors transition from a fast-detaching state to a slow-detaching state. This model, described in the methods, gives a much better fit (adjusted $R^2 = 0.95$, Figure 7B) and a detachment rate at zero force of $k_1^0 \sim (1.2 \pm 0.1) \cdot 10^{-4}$s^{-1}. These results indicate that a conformational change of LacI occurs when it binds the operator.

DISCUSSION

Our method permits direct monitoring of interactions between LacI and DNA at the single molecule level with unprecedented high resolution. Our data largely agrees with the well-established model of allosteric regulation pioneered by Jacob and Monod (3) and gives new insights into the still debated model of facilitated diffusion for DNA-binding proteins (7). It is well established that LacI switches between two conformations that bind Lac operators either strongly, to block transcription of the lac operon (LacI-R), or weakly, to allow lac operon transcription (LacI-R*).

In our experiments, we observed three interaction modalities of single LacI molecules with DNA: strongly bound (long interactions), weakly bound (short interactions) and sliding along DNA (Figure 2). We attribute long and short interactions to LacI-R and LacI-R* conformations, respectively. Such hypothesis is confirmed by the fact that long interactions are localized on the two O1 operator sequences (Figures 2 and 3). Moreover, IPTG accelerates the detachment rate of long interactions about 25-fold, whereas it does not influence the detachment kinetics of short interactions (Figure 4). This observation indicates that IPTG induces the transition from LacI-R to LacI-R* and, consequently, accelerates the detachment of the protein from the operator. Residence times of LacI on DNA measured in living bacteria in the presence of IPTG (0.3–5 ms) (13) are in good agreement with our measurement of the detachment rate of short interactions, extrapolated at zero force ($k_2^0 = 350 \pm 90$ s^{-1}). On the other hand, the detachment rate of long interactions at zero force $k_1^0 \sim (1.2 \pm 0.1) \cdot 10^{-4}$ s^{-1} is in good agreement with the rates previously measured for LacI detaching from O1 (31). IPTG, not only nearly abolishes long interactions with the operator, but also strongly reduces sliding. We, therefore, attribute sliding of LacI along DNA to the LacI-R conformation. The fact that LacI slides on DNA only in its active conformation might be an important regulatory mechanism *in vivo* to minimize DNA crowding when the repressor is inactive. In this picture, LacI-R slides along nonspecific sequences and, occasionally, switches from sliding to specific binding on the operator, and *vice versa*, as directly observed in our experiments (Figure 2B and Supplementary Figure S4). A model that recapitulates the relationship between LacI conformations with short, long, and sliding interactions with DNA is depicted in Figure 8.

From LacI sliding on DNA, we measured 1D diffusion coefficients varying over a large range from $1 \cdot 10^4$ to $5 \cdot 10^6$ nm^{2}s^{-1}, which overlaps well with the range of values previously reported from single molecule measurements (12,13,35). The distribution of diffusion coefficient that we measure is peaked around $4.1 \cdot 10^5$ nm^{2}s^{-1}, a value about one order of magnitude larger than the average values measured *in vitro* at low salt concentration ($2.1 \cdot 10^4$ nm^{2}s^{-1} (12); $4.6 \cdot 10^4$ nm^{2}s^{-1} (13)). Experiments performed in living cells, however, show diffusion constants similar to the ones that we measure: Caccianini *et al.* found diffusion constants with an apparent bimodal distribution with the first peak centered around $5 \cdot 10^6$ nm^{2}s^{-1}, which they attributed to proteins diffusing in the nucleoplasm, and the second one centered around $3 \cdot 10^5$ nm^{2}s^{-1}, which they interpreted as the
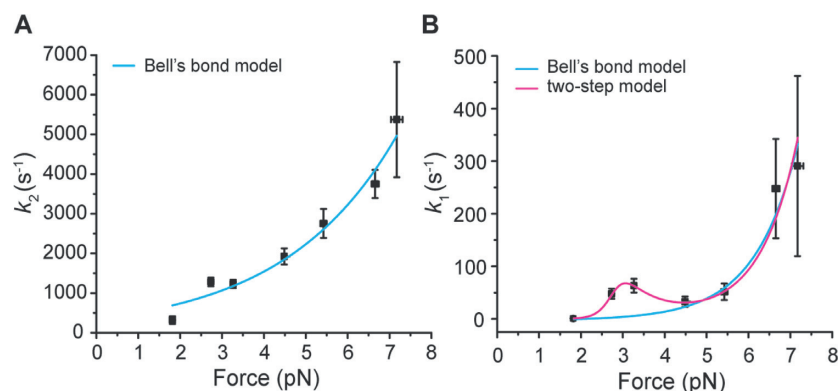
Figure 7. Effect of force on the kinetics of local interactions. (**A**) Detachment rate of short interactions (k_2) as a function of force. Cyan curve is the fitting curve with the Bell's bond model $k_2(F) = k_2^0 \exp(d_2 F / k_B T)$, which gives $k_2^0 = 350 \pm 90$ s^{-1} and $d_2 = 1.5 \pm 0.2$ nm. (**B**) Detachment rate of long interactions with the operator (k_1). k_1 is well fitted by a two-step model (magenta, adjusted $R^2 = 0.95$), whereas the Bell's bond model cannot properly fit data (cyan, adjusted $R^2 = 0.3$). Fit parameters of the two-step model are (see 'Materials and Methods' section and Supplementary Figure S2): $k_{IU}^0 = (1.2 \pm 0.1) \cdot 10^{-4}$ s^{-1}, $d_{IU} = (19.9 \pm 0.1)$ nm, $k_{OU}^0 = (8 \pm 3) \cdot 10^{-4}$ s^{-1}, $d_{OU} = (4.4 \pm 0.3)$ nm, $k_{IO}^0 = (9 \pm 1) \cdot 10^{-7}$ s^{-1}, $d_{IO} = (19 \pm 1)$ nm, $k_{OI}^0 = 23 \pm 11$ s^{-1}, $d_{OI} = (5.1 \pm 0.6)$ nm.
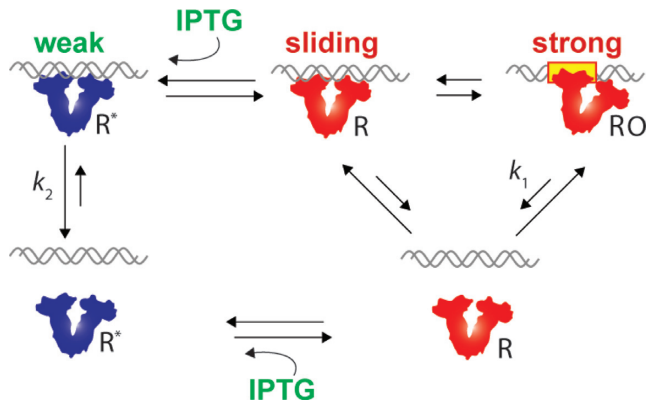

Figure 8. A model for allosteric regulation and target-search mechanism of LacI. LacI can adopt two main conformations, LacI-R* (blue), which weakly interacts with DNA and LacI-R (red) with high affinity for the operator. In the LacI-R conformation, the protein also slides along nonspecific sequences. IPTG drives the equilibrium toward the LacI-R* conformation, inhibiting LacI repression by strongly reducing both sliding and long interactions with the operator. k_1 and k_2 respectively represent detachment rates of long and short local interactions. Arrow lengths are representative of the equilibrium constant between states.

proteins interacting with DNA (35). Elf et al measured a similar apparent diffusion constant of $4 \cdot 10^5$ nm^{2}s^{-1} in living bacteria (13). It is therefore possible that the large diffusion constant that we measure derives from the high salt concentration used in our experiments, close to the one of living cells. However, further experiments would be required to assess this point. It is possible that the large variability of the 1D diffusion coefficient of LacI on DNA observed here and in previous studies (12,35) might be a consequence of a complex array of conformations that Lac repressor can experience on nonspecific DNA sequences. Therefore, the two-conformation scheme, with LacI switching from a low-affinity LacI-R* to a high-affinity LacI-R conformation, might be a simplification of a possibly much richer energy potential in which LacI moves between a series of intermediate states, as also suggested by other studies (36). High-

resolution mapping of LacI sliding indicates that the 1D diffusion coefficient of LacI along DNA is sequence dependent. The correlation between sliding velocity at different time points is on average 0.77 ± 0.02, significantly different from that obtained on different DNA segments (0.19 ± 0.07). Our observations agree with current models (34) and sequence-dependent sliding observed for p53 (37) and, to our knowledge, is the first direct observation of sequence-dependent sliding of the *lac* repressor protein.

Finally, our data suggest that recognition of the target sequence and transition from sliding to strong binding to the operator requires a conformational change of LacI. A two-step model for the binding of proteins to target sequences is largely accepted in the literature, in which the first step corresponds to the protein binding to non-specific sequences and the second to the protein binding the cognate sequence (34,36,38). We observe LacI scanning over the operator several times before strongly binding to it. This is evident in Figures 2, 5 and Supplementary Figure S4, where sliding overlaps with the position of the operators in the DNA. This finding has been also suggested by previous studies *in vivo* (14) and indicates that a conformational change is required for binding of LacI to the operator. The exponential distribution of the sliding time before binding to an operator (data not shown) indicates that this transition is a stochastic process. Interestingly, we found that the molecular bond between LacI and the operator is a catch-bond, which requires two conformations of LacI to accurately fit our data. Intriguingly, this result suggests that this two LacI conformations might be the same indicated by the aforementioned two-step models for the binding of LacI to the operator. The large distance parameters that we obtain from our model (Supplementary Figure S2) also suggest that recognition of the target sequence by LacI might require large scale rearrangements of the tetrameric complex, as previously observed by Taraban *et al.* (39) and Rutkauskas *et al.* (40).

SUPPLEMENTARY DATA

Supplementary Data are available at NAR Online.

REFERENCES

1. Riggs,A.D., Bourgeois,S. and Cohn,M. (1970) The lac represser-operator interaction. 3. Kinetic studies. *J. Mol. Biol.*, **53**, 401–417.
2. Lewis,M. (2005) The lac repressor. *C. R. Biol.*, **1328**, 521–548.
3. Lewis,M. (2013) Allostery and the lac operon. *J. Mol. Biol.*, **425**, 2309–2316.
4. Lewis,M., Chang,G., Horton,N.C., Kercher,M.A., Pace,H.C., Schumacher,M.A., Brennan,R.G. and Lu,P. (1996) Crystal structure of the lactose operon repressor and its complexes with DNA and inducer. *Science*, **271**, 1247–1254.
5. Gilbert,W. and Muller-Hill,B. (1966) Isolation of the lac repressor. *Proc. Natl. Acad. Sci. U.S.A.*, **56**, 1891–1898.
6. Xie,X.S., Choi,P.J., Li,G.-W., Lee,N.K. and Lia,G. (2008) Single-molecule approach to molecular biology in living bacterial cells. *Annu. Rev. Biophys.*, **37**, 417–444.
7. Monico,C., Capitanio,M., Belcastro,G., Vanzi,F. and Pavone,F.S. (2013) Optical methods to study protein-DNA interactions in vitro and in living cells at the single-molecule level. *Int. J. Mol. Sci.*, **14**, 3961–3992.
8. Von Hippel,P.H. and Berg,O.G. (1989) Facilitated target location in biological systems. *J. Biol. Chem.*, **264**, 675–678.
9. Delbruck,G. and Adam,M. (1968) Reduction of dimensionality in biological diffusion processes. In: Rich,A and Davidson,N (eds). *Structural Chemistry in Molecular Biology*. Freeman, San Francisco, pp. 198–215.
10. Capitanio,M. and Pavone,F.S. (2013) Interrogating biology with force: single molecule high-resolution measurements with optical tweezers. *Biophys. J.*, **105**, 1293–1303.
11. Skinner,G.M., Baumann,C.G., Quinn,D.M., Molloy,J.E. and Hoggett,J.G. (2004) Promoter binding, initiation, and elongation by bacteriophage T7 RNA polymerase. A single-molecule view of the transcription cycle. *J. Biol. Chem.*, **279**, 3239–3244.
12. Wang,Y.M., Austin,R.H. and Cox,E.C. (2006) Single molecule measurements of repressor protein 1D diffusion on DNA. *Phys. Rev. Lett.*, **97**, 048302.
13. Elf,J., Li,G.-W. and Xie,X.S. (2007) Probing transcription factor dynamics at the single-molecule level in a living cell. *Science*, **316**, 1191–1194.
14. Hammar,P., Leroy,P., Mahmutovic,A., Marklund,E.G., Berg,O.G. and Elf,J. (2012) The lac repressor displays facilitated diffusion in living cells. *Science*, **336**, 1595–1598.
15. Candelli,A., Wuite,G.J. and Peterman,E.J. (2011) Combining optical trapping, fluorescence microscopy and micro-fluidics for single molecule studies of DNA-protein interactions. *Phys. Chem. Chem. Phys.*, **13**, 7263–7272.
16. Monico,C., Belcastro,G., Capitanio,M., Vanzi,F. and Pavone,F.S. (2011) Combined optical trapping and nanometer-precision localization for the single-molecule study of DNA-binding proteins. In: *2011 International Workshop on Biophotonics*. IEEE, Parma, pp. 1–3.
17. Monico,C., Belcastro,G., Vanzi,F., Pavone,F.S. and Capitanio,M. (2014) Combining single-molecule manipulation and imaging for the study of protein-DNA interactions. *J. Vis. Exp.*, **90**, e51446.
18. Gardini,L., Capitanio,M. and Pavone,F.S. (2015) 3D tracking of single nanoparticles and quantum dots in living cells by out-of-focus imaging with diffraction pattern recognition. *Sci. Rep.*, **5**, 16088
19. Capitanio,M., Canepari,M., Maffei,M., Beneventi,D., Monico,C., Vanzi,F., Bottinelli,R. and Pavone,F.S. (2012) Ultrafast force-clamp spectroscopy of single molecules reveals load dependence of myosin working stroke. *Nat. Methods*, **9**, 1013–1019.
20. Zhan,H., Swint-Kruse,L. and Matthews,K.S. (2006) Extrinsic interactions dominate helical propensity in coupled binding and folding of the lactose repressor protein hinge helix. *Biochemistry*, **45**, 5896–5906.
21. Capitanio,M., Canepari,M., Cacciafesta,P., Lombardi,V., Cicchi,R., Maffei,M., Pavone,F.S. and Bottinelli,R. (2006) Two independent mechanical events in the interaction cycle of skeletal muscle myosin with actin. *Proc. Natl. Acad. Sci. U. S. A.*, **103**, 87–92.
22. Gardini,L., Tempestini,A., Pavone,F.S. and Capitanio,M. High-speed optical tweezers for the study of single molecular motors. In: Lavelle,C (ed). *Molecular Motors: Methods and Protocols, Second Edition*. Methods in Molecular Biology, Springer US.
23. Smith,S.B., Cui,Y. and Bustamante,C. (1996) Overstretching B-DNA: the elastic response of individual double-stranded and single-stranded DNA molecules. *Science*, **271**, 795–799.
24. Hsieh,M. and Brenowitz,M. (1997) Comparison of the DNA association kinetics of the Lac repressor tetramer, its dimeric mutant LacI adi, and the native dimeric Gal repressor. *J. Biol. Chem.*, **272**, 22092–22096.
25. Capitanio,M., Cicchi,R. and Pavone,F.S. (2005) Position control and optical manipulation for nanotechnology applications. *Eur. Phys. J. B.*, **46**, 1–8.
26. Capitanio,M., Normanno,D. and Pavone,F.S. (2004) High-precision measurements of light-induced torque on absorbing microspheres. *Opt. Lett.*, **29**, 2231–2233.
27. Capitanio,M., Romano,G., Ballerini,R., Giuntini,M., Pavone,F.S., Dunlap,D. and Finzi,L. (2002) Calibration of optical tweezers with differential interference contrast signals. *Rev. Sci. Instrum.*, **73**, 1687–1696.
28. Capitanio,M., Gardini,L. and Pavone,F.S. (2013) Analysis of single-molecule mechanical measurements with high spatio-temporal resolution. In: Dholakia,K and Spalding,GC (eds). *Proceedings of SPIE—The International Society for Optical Engineering*. International Society for Optics and Photonics, San Diego, Vol. **8810**, pp. 881034.
29. Nolting,B. (1999) *Protein Folding Kinetics—Biophysical Methods second*. Springer, Berlin.
30. Winter,R.B. and Von Hippel,P.H. (1981) Diffusion-driven mechanisms of protein translocation on nucleic acids. 2. The Escherichia coli lac repressor-operator interaction: equilibrium measurements. *Biochemistry*, **20**, 6948–6960.
31. Sharp,K.A. (2011) Allostery in the lac operon: Population selection or induced dissociation? *Biophys. Chem.*, **159**, 66–72.
32. Slutsky,M. and Mirny,L.A. (2004) Kinetics of protein-DNA interaction: facilitated target location in sequence-dependent potential. *Biophys. J.*, **87**, 4021–4035.
33. Jackson,M.B. (2006) *Molecular and Cellular Biophysics*. 2006th edn. Cambridge University Press, Cambridge.
34. Tafvizi,A., Mirny,L.A. and van Oijen,A.M. (2011) Dancing on DNA: kinetic aspects of search processes on DNA. *Chem. Phys. Chem.*, **12**, 1481–1489.
35. Caccianini,L., Normanno,D., Izeddin,I. and Dahan,M. (2015) Single molecule study of non-specific binding kinetics of LacI in mammalian cells. *Faraday Discuss.*, **184**, 393–400.
36. Kalodimos,C.G. (2004) Structure and flexibility adaptation in nonspecific and specific protein-DNA complexes. *Science*, **305**, 386–389.
37. Leith,J.S., Tafvizi,A., Huang,F., Uspal,W.E., Doyle,P.S., Fersht,A.R., Mirny,L.A. and van Oijen,A.M. (2012) Sequence-dependent sliding kinetics of p53. *Proc. Natl. Acad. Sci. U.S.A.*, **109**, 16552–16557.
38. Berg,O.G., Winter,R.B. and Von Hippel,P.H. (1981) Diffusion-driven mechanisms of protein translocation on nucleic acids. 1. Models and theory. *Biochemistry*, **20**, 6929–6948.
39. Taraban,M., Zhan,H., Whitten,A.E., Langley,D.B., Matthews,K.S., Swint-Kruse,L. and Trewhella,J. (2008) Ligand-induced conformational changes and conformational dynamics in the solution structure of the lactose repressor protein. *J. Mol. Biol.*, **376**, 466–481.
40. Rutkauskas,D., Zhan,H., Matthews,K.S., Pavone,F.S. and Vanzi,F. (2009) Tetramer opening in LacI-mediated DNA looping. *Proc. Natl. Acad. Sci. U.S.A.*, **106**, 16627–16632.